AD-A078 323 DEFENCE RESEARCH ESTABLISHMENT VALCARTIER (QUEBEC) F/G 17/8
PULSED TEA-CO2 LASER RADAR WITH HETERODYNE DETECTION.(U)
AUG 78 J M CRUICKSHANK
UNCLASSIFIED DREV-R-4116/78 NL

| OF |
AD A078323

END
DATE FILMED
1-80
DDC

UNCLASSIFIED

(3)

CRDV RAPPORT 4116 78
DOSSIER: 3633H-006
AOUT 1978

LEVEL II

DREV REPORT 4116 78
FILE: 3633H-006
AUGUST 1978

# PULSED TEA-$CO_2$ LASER RADAR WITH HETERODYNE DETECTION

J.M. Cruickshank









Centre de Recherches pour la Défense
Defence Research Establishment
Valcartier, Québec

BUREAU - RECHERCHE ET DEVELOPPEMENT
MINISTÈRE DE LA DÉFENSE NATIONALE
CANADA

NON CLASSIFIÉ

RESEARCH AND DEVELOPMENT BRANCH
DEPARTMENT OF NATIONAL DEFENCE
CANADA

CRDV R-4116/78
DOSSIER: 3633H-006

UNCLASSIFIED

(14) DREV-R-4116/78
FILE: 3633H-006

(3)



(9) Rept. for Jan 76 - Nov 77,

(6) PULSED TEA-$CO_2$ LASER RADAR WITH HETERODYNE DETECTION.

(10) by

J.M. Cruickshank

(11) Aug. 78

(12) 20



CENTRE DE RECHERCHES POUR LA DEFENSE

DEFENSE RESEARCH ESTABLISHMENT

VALCARTIER

Tel: (418) 844-4271

Québec, Canada

August/août 1978

NON CLASSIFIE

404 945

AB

## RESUME

La possibilité de mesurer la distance de cibles à l'aide d'un télémètre laser comportant un transmetteur à laser hybride $CO_2$ TEA et un récepteur à détection hétérodyne a été démontrée expérimentalement. Dans ce rapport, nous décrivons le système et en donnons les principes de fonctionnement et les performances. On donne également les résultats obtenus lors de mesures de distance effectuées sur des cibles éloignées, d'une part, jusqu'à 5 km et dont les caractéristiques avaient été mesurées au préalable et d'autre part, jusqu'à 32 km sur des cibles naturelles. En dernier lieu, nous considérons brièvement la possibilité d'utiliser un transmetteur à laser $CO_2$ TEA avec les systèmes de radar optiques capables de déceler et poursuivre des cibles rapides. (NC)

## ABSTRACT

Ranging has been demonstrated with an experimental laser rangefinder employing a hybrid TEA-$CO_2$ laser transmitter and a heterodyne-detection receiver. A description of the system, including its operating principles and performance characteristics, is presented. Ranging results are given to 5 km on targets with previously measured characteristics and to 32 km on natural targets. The application of TEA-$CO_2$ laser transmitters in optical radar systems capable of detecting and tracking high speed targets is briefly discussed. (U)

TABLE OF CONTENTS

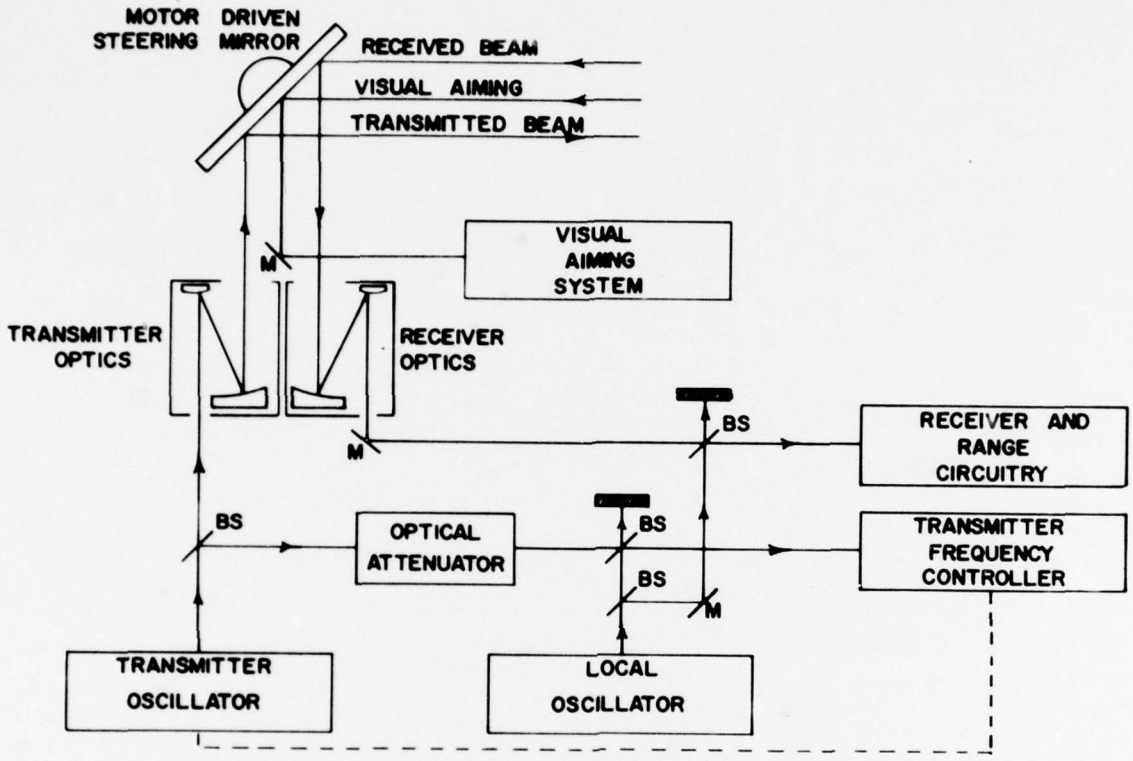


FIGURE 1 - 10.6-μm Laser Radar with Heterodyne Detection

## 1.0 INTRODUCTION

Although laser radars using heterodyne detection have been previously reported with various types of transmitters [1-4], the system studied in this report is unique in that a hybrid TEA-$CO_2$ laser [5-8] serves as the transmitter and that the overall system is similar to a pulsed radar at microwave frequencies. Heterodyne detection has been chosen over direct detection for this system to achieve a high receiver-sensitivity. With a signal-to-noise ratio sufficient to give a 95 percent probability of detection with a low false alarm rate, a heterodyne receiver should be able to detect signals a factor $10^2$ to $10^3$ weaker than the equivalent direct detection receiver. A high receiver-sensitivity lowers the requirements on laser peak power and opens the way for high-repetition-rate systems. An added advantage of heterodyne detection with moving targets is the availability of a doppler frequency shift of 189 KHz/m/s of radial velocity. This doppler frequency shift is of major significance for the discrimination of moving targets from a stationary background or atmospheric backscatter, especially in conditions of fog, rain, and snow.

The work described in this document was performed at DREV between January 1976 and November 1977 under PCN 33H06 (formerly PCN 34D05), entitled: "Study of 10.6-μm ladars".

## 2.0 SYSTEM DESCRIPTION

The experimental laser radar system can be divided into the basic sub-systems shown in Fig. 1. It consists of the transmitter oscillator, transmitter frequency controller, local oscillator, receiver, beam optics, and visual aiming system. Figures 2 and 3 show the laboratory apparatus except for the final motor driven steering mirror which was mounted in an observatory dome directly above the laboratory.

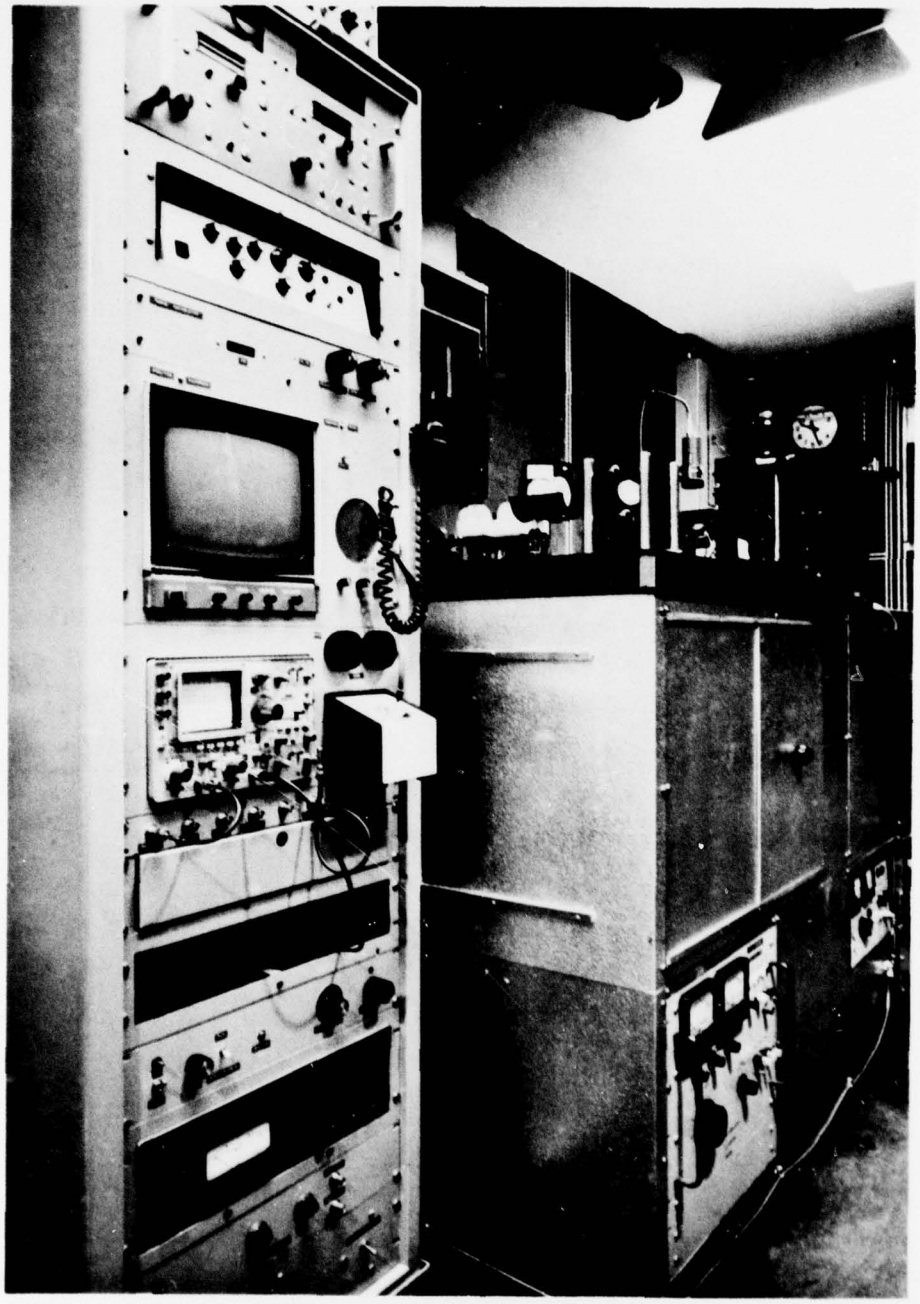

FIGURE 2 - Laser Radar Apparatus

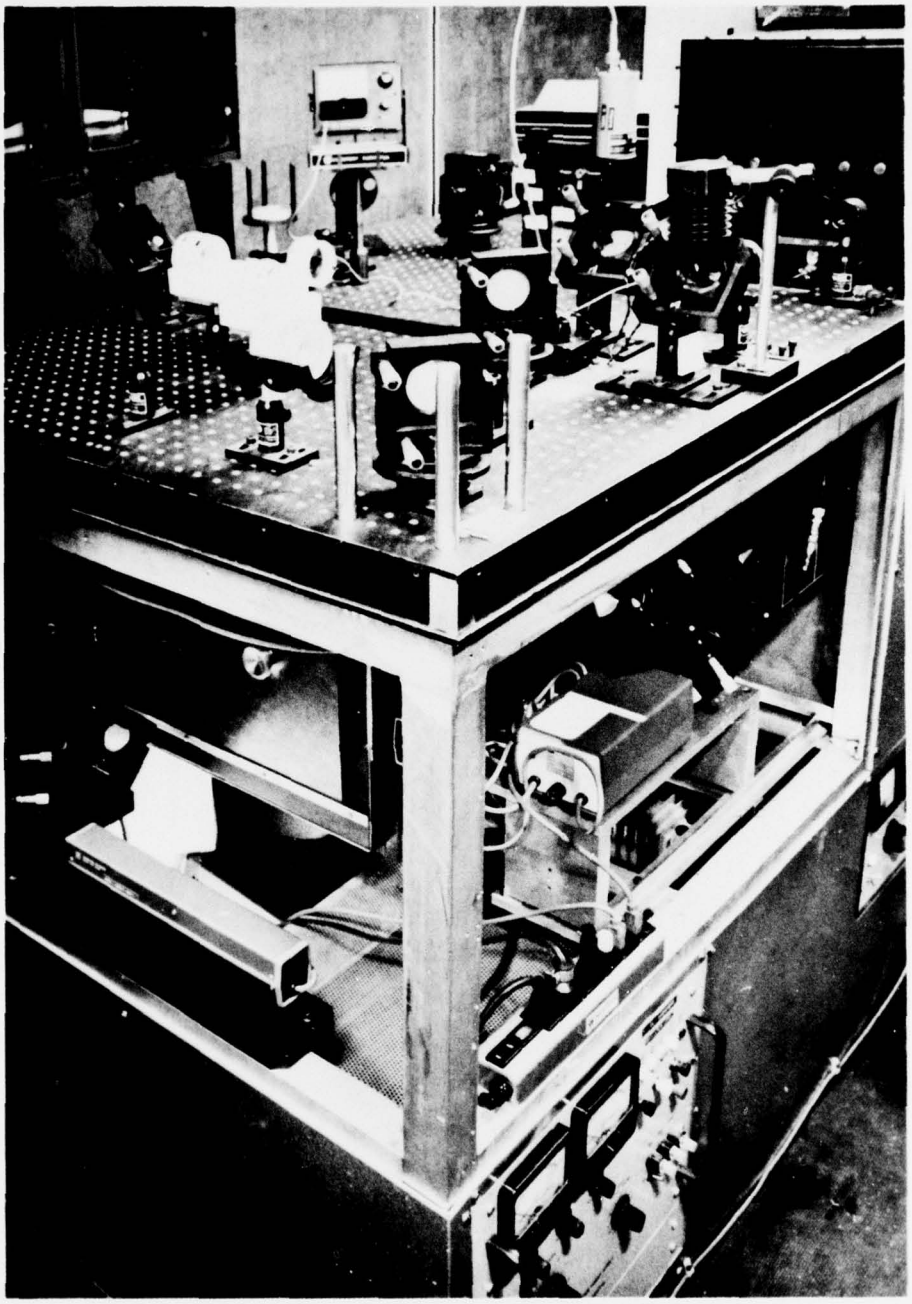

FIGURE 3 - Optical Bench with Transmitter and Local Oscillator

The hybrid transmitter oscillator consists of a Lumonics 102 TEA-$CO_2$ gain section and a low-pressure gain section with a 2.5-cm-diameter bore in a common optical cavity formed from a 10-m radius of curvature Littrow-mounted reflection grating (75 lines/mm), and a 70-percent-reflectivity flat output window. The output window was limited with a 10-mm iris and was mounted in a piezoelectric translator with a 12μm excursion range. Both gain sections operated on a premixed $He:CO_2:N_2$ (84:10:6) gas mixture with the TEA gain section at atmospheric pressure and the CW low-pressure section at 10 torr. The transmitter with a 298-cm optical cavity produced a single frequency tunable output with a CW output power of 1 W and a pulsed peak power output of 400 kW at the rate of one pulse per second.

The local oscillator was a sealed off $CO_2$ laser, frequency stabilized to the centre of the P(20) transition at 10.59 μm with a lock-in stabilizer and a 2-m radius of curvature diffraction grating.

The receiver consisted of a Germanium focussing lens, a 10.6-μm detector, an i-f amplifier, an envelope detector and signal displays. The focal length of the lens was chosen such that the diameter of the Airy disk formed by focussing the 1-cm-diameter beam from the telescope approximated the dimension of the HgCdTe photovoltaic detector element. The preamplifier, designed to have a low input impedance and provide a constant voltage bias to the detector, was tuned to a 12.5-MHz centre frequency. With 0.5 mW of local oscillator power focussed on the detector element, the shot noise produced by the detector was greater than the other noise sources associated with the detector and preamplifier. The linear envelope-detector demodulated the i-f signal and provided the stop pulse for the range calculator. The range calculator was basically a gated counter driven with a 14.99 MHz crystal controlled clock. Each clock pulse counted in the time interval from the transmitter pulse output to the received echo corresponded to 10 m in range. Additional gates were provided to eliminate electrical interference from the discharge of the laser transmitter and to prevent atmospheric backscatter

at close ranges from triggering the stop threshold of the calculator. The characteristics of either the i-f or demodulated signal could be monitored on an oscilloscope.

Due to the complexity of the problem of eliminating changes in the laser cavity length resulting from thermal expansion and mechanical vibration, electronic techniques were developed to provide the required transmitter frequency stabilization. The main components of the frequency controller are shown in Fig. 4. A portion of the output beam from the transmitter oscillator was deviated to the frequency controller with a NaCl beam-splitter. $CaF_2$ windows, providing an additional 60-dB attenuation, were placed in this beam to prevent the 400-kW-output pulse from damaging the 10.6-μm detector but permitted enough of the CW output to reach the detector to provide a good signal-to-noise ratio for frequency stabilization when mixed with the output from the local oscillator. Frequency stabilization of the transmitter output pulse was obtained in the following manner. The output mirror of the hybrid laser transmitter was driven back and forth with a piezoelectric translator controlled by a ramp generator. The ramp voltage had a 20-ms rise-time and the cavity length changed by slightly more than half a wavelength. For each half-wavelength excursion of the cavity length, the CW output frequency ($f_o$) of the transmitter was driven through its full operating range which is equal to the intercavity-mode spacing of 50.3 MHz. Because the local oscillator frequency ($f_{lo}$) was stabilized at the centre of the laser transition, the frequency at the input of the frequency discriminator $f_s=f_o-f_{lo}$ remained between zero and 25.2 MHz. In addition, for each sweep of the cavity length, any given value of the frequency $f_s$ was produced twice; once for $f_o<f_{lo}$ and once for $f_o>f_{lo}$. Based on a fundamental principle of resonators (increasing cavity length decreases the frequency of a given cavity mode) it was known that, during a sweep that increased the cavity length, $f_s$ was increasing for $f_o<f_{lo}$ and decreasing for $f_o>f_{lo}$. The combination of the frequency discriminator and trigger circuit were

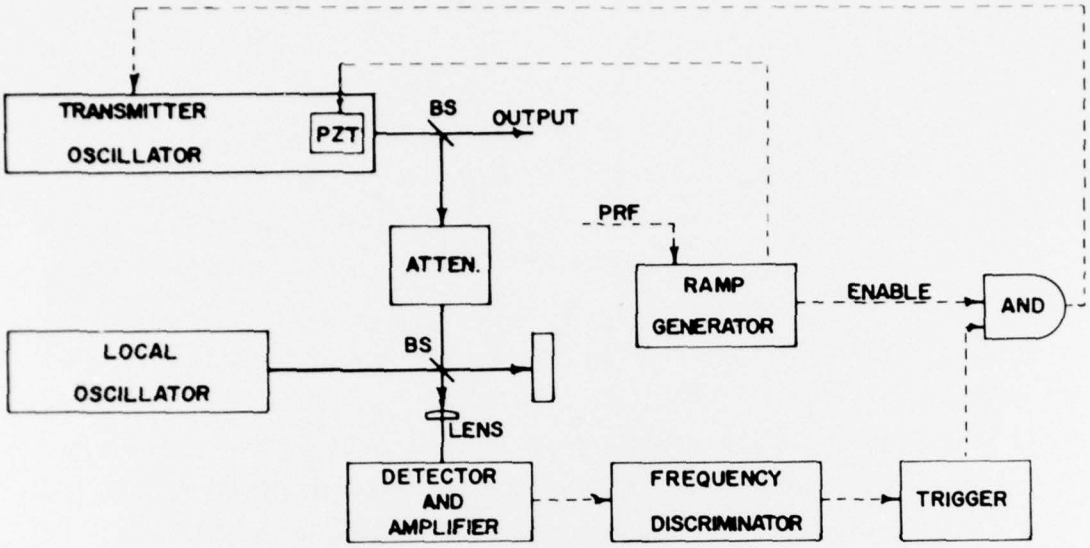


FIGURE 4 - Transmitter Frequency Controller

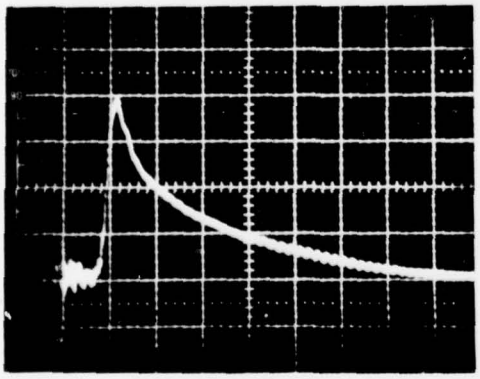

TRANSMITTER OUTPUT PULSE

Vert: 105 KW/div.

Hor : 0.5μs/div.

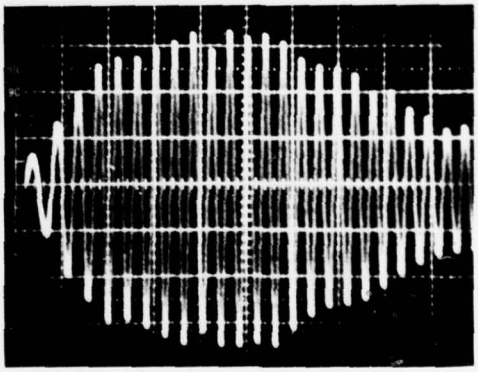

RECEIVED PULSE AT
OUTPUT OF I.F. AMPLIFIER

Hor : .2μ/div.

FIGURE 5 - Pulse Shape and Frequency Characteristics

therefore designed to give a trigger output pulse only when $f_s$ was increasing and equal to a predetermined value. This trigger pulse was then AND-gated with an enable signal from the ramp generator during the period of increasing cavity length, and the total circuit configuration resulted in the TEA laser section being pulsed when $f_s$ was equal to the preset given value and for only $f_o < f_{lo}$.

The transmitting and receiving "antennae" were two identical 10-cm-diameter folded off-axis beam expanders. The laser output beam was expanded a factor of 10 prior to transmitting, and the diameter of the collected echo-signal beam was reduced from 10 cm to 1 cm before being superimposed on the local oscillator beam. The full-angle field of view of the receiver, essentially determined by the diffraction limit of the input optics, was taken to be about 0.1 mrad. The 10.6-μm optics as well as the visual aiming system were directed to the target by means of a 40-cm-diameter motor-driven steering mirror with an aiming resolution of < 1 μrad. The infrared beam was aimed by means of the visual aiming system consisting of a riflescope, a motor-driven dove prism for image rotation and a video camera. With this system, cross hairs and an erect image were displayed on a video monitor for all azimuth positions of the final steering mirror.

## 3.0 PERFORMANCE

Using both measured and estimated parameters for the system, a calculated theoretical ranging performance was compared to the experimental results. This comparison could be useful for optimizing the present system, and for predicting the performance of any future system.

The transmitter output pulse shape as recorded with a photon drag detector is shown in Fig. 5(a). The energy in this pulse was measured with a joulemeter to be 380 mJ. The frequency characteristics of the output pulse were obtained by recording the signal return from

a target at the output of the i-f amplifier of the receiver. Fig. 5(b) is a typical received pulse. It has about a 1-MHz frequency chirp in its rise. In the microsecond following this initial chirp, both the chirp and the pulse-to-pulse frequency-jitter of the i-f signal were less than could be measured from a photograph (i.e. <500 KHz) for a given adjustement of the transmitter frequency controller. The frequency of the output pulse was typically 1 MHz lower than the CW laser frequency $f_o$ at the moment the TEA laser section was triggered. The comparison of the pulse envelope shape at the output of the receiver i-f with the pulse shape of the transmitter output indicates that the bandwidth of the receiver does not pass the initial spike of the transmitter pulse. Therefore, in calculations to determine the theoretical signal-to-noise ratio (S/N-ratio), the output power has been taken as 70 percent of the peak value measured.

The divergence of the transmitter output was measured by focussing the output beam with a high-quality parabolic mirror onto a detector limited by an iris. It was found that approximately 25 percent of the total output fell within an angle equal to the receiver nominal field-of-view of 0.1 mrad. The far-field beam divergence was also measured at a site 5 km from the laser transmitter. The beam produced by the CW section of the hybrid transmitter was chopped and scanned in angle across a single HgCdTe photodiode at the focus of a short-focal-length lens. The measurement indicated a FWHM divergence of 0.13 mrad. Under conditions of low atmospheric turbulence and at the angular position of maximum signal, the standard deviation on the amplitude of the recorded signal was 0.26 of the mean value. With conditions of higher turbulence, due mainly to the large temperature differential existing in the region of the final steering mirror when the exterior temperature was low, the standard deviation on the recorded signal was 0.52 of the mean value. By integrating in two dimensions under the beam profile curve, it was found that the power contained in the central 0.1 mrad was approximately 25 percent of the total. This divergence

measurement is therefore consistent with the earlier measurement which used irises and a long-focal-length mirror. To account for both the transmitter divergence and the receiver bandwidth characteristics in S/N-ratio calculations, the transmitter power $P_T$ was taken as 70 kW within a divergence angle of 0.1 mrad.

The echo S/N-ratio experimentally obtained from known targets was compared to the S/N-ratio calculated from the system parameters. Targets of interest were of both the extended and point types and an expression for S/N-ratio was calculated for each. A target was classified as extended when it subtended an angle greater than the receiver field of view. For a laser radar directed at an extended target, the signal power received can be given as:

$$P_s = \frac{P_T A_r T \rho}{\pi R^2 \times 10^6} \times 10^{-0.2\beta R} \qquad (1)$$

where $P_T$ = Transmitter power radiating within receiver field of view in W

$A_r$ = Area of receiver optics in $m^2$

$T$ = Transmittance of optical system

$\rho$ = Target reflectance

$\beta$ = Attenuation coefficient in dB/km

$R$ = Target range in km

For heterodyne detection with the dominating noise source being the shot noise produced by the local oscillator power, the power S/N-ratio is generally given as [9]:

$$\frac{S}{N} = \frac{\eta P_s}{h \nu \Delta f} \qquad (2)$$

where $P_s$ = The signal power available on the detector in watts with the same polarization as the local oscillator [10]

$\eta$ = Effective quantum efficiency determined by the detector quantum efficiency and the matching of the signal and

local oscillator beams to the detector dimensions [11-13]

$h$ = Planck's constant ($6.6 \times 10^{-34}$ joule-sec)

$\nu$ = Optical frequency of signal in Hz

$\Delta f$ = Noise bandwidth of detector and intermediate frequency amplifier in Hz

Substituting Eq. 1 into Eq. 2 for $P_s$ gives:

$$\frac{S}{N} = K_{ext} \frac{\rho}{R^2} \times 10^{-0.2\beta R} \tag{3}$$

where $$K_{ext} = \frac{\eta T P_T A_r}{h \nu \Delta f \pi \times 10^6}$$

$K_{ext}$ is a system constant for extended targets which is determined entirely by the characteristics of the laser radar equipment. Similarly for point targets the S/N-ratio can be defined as:

$$\frac{S}{N} = K_p \frac{\sigma}{R^4} \times 10^{-0.2\beta R} \tag{4}$$

where $$K_p = \frac{\eta T P_T A_r}{h \nu \Delta f \theta_t{}^2 \pi^2 \times 10^{12}}$$

and where

$\theta_t$ = The full angle transmitter divergence in radians that contains the transmitter power $P_T$

$\sigma$ = Radar cross section

A flat diffuse plate reflector at normal incidence has $\sigma = 4\rho A_t$ where $A_t$ is the physical area of the target in $m^2$. For the described system the above parameters were determined as:

$\eta \simeq 0.2$, $\Delta f = 4.1$ MHz, $T \simeq 0.5$, $P_T = 70$ kW, $A_r = 7.9 \times 10^{-3}$ $m^2$,

$\theta_t = 0.1$ mrad, $K_{ext} = 2.29 \times 10^8$ $km^2$ and $K_p = 7.15 \times 10^9$ $km^4/m^2$

Radar returns were studied from targets of known size and reflectivity, as well as from natural objects visible from the site of the ladar. The results given are preliminary and it is anticipated that improvements will result with continuing work and system modifications.

The first target was an extended sandblasted aluminum plate fixed to a water tower 1.8 km away. With a large number of transmitter pulses, the mean S/N-ratio was measured at $3.8 \times 10^6$ (65.8 dB) and the standard deviation at 0.89 of the mean value. The maximum S/N-ratio observed on any pulse during the measurement was $11.5 \times 10^6$ (70.6 dB). Substituting into Eq. 3 the value for $K_{ext}$, an estimated value of atmospheric attenuation of 1 dB/km for the day of the measurement, and the plate diffuse-reflectivity of 0.8, gives the calculated S/N-ratio of $2.47 \times 10^7$ (73.9 dB). This preliminary measurement therefore gave a 8.1 dB difference between the calculated and measured S/N-ratio.

The measured point target was a 10 cm × 10 cm sandblasted aluminum plate 4.92 km away. The target plate was held perpendicular to the beam and clear of obstructions with small-diameter strings from two poles. The path to the target at an average height of 15 m from the ground passed over fields, trees, roads and buildings. Objects behind the target were at a sufficient range to avoid confusion between the target-signal return and the background return. The mean S/N-ratio observed was $7.7 \times 10^3$ (38.9 dB) and the standard deviation was of equal magnitude. The maximum single pulse return gave an S/N-ratio of $3.9 \times 10^4$ (45.9 dB). There is little doubt that the atmospheric turbulence, especially in the region of the opening to the exterior environment, and the vibrating motion of the whole laboratory contributed to the production of the large signal-power variations. If one uses the value

given for $K_p$, an assumed attenuation of $\beta$=0.6 dB/km on the day of the measurement and a target diffuse-reflectivity of $\rho$=0.8, Eq. 4 gives the calculated S/N-ratio of $1.0 \times 10^5$ (50 dB). In this case, the average measured S/N-ratio is 11.1 dB less than that calculated. Extrapolation of the results obtained on small targets indicates that the experimental system could detect a target of $4 \times 10^{-4} m^2$ radar cross section at 5 km with a mean S/N-ratio of 20 dB under low atmospheric attenuation, or a target of $4 \times 10^{-2}$ $m^2$ radar cross section at 5 km with a 15 dB S/N-ratio when the atmospheric attenuation is as high as 3 dB/km such as found in light fog and light rain.

Ranging was also performed on several natural or uncalibrated targets. Under low atmospheric-attenuation conditions, an antenna tower with a width of 45 cm and located at 6.9 km gave returns with an average S/N-ratio of 40 dB. A house roof at 9 km gave an S/N-ratio of 25 dB. The maximum range obtainable from this location on days of low atmospheric attenuation (example: clear sky, temperature 12°C, relative humidity 64%) was 32 km on a tree-covered mountain. The S/N-ratio was high enough to give range results for >70% of the returns. As the water content in the air increased (example: temperature 19.1°C and relative humidity 64%) this maximum range was reduced to 16 km on another mountain.

## 4.0 CONCLUSIONS

The operation of an experimental TEA-$CO_2$ laser rangefinder with heterodyne detection has been demonstrated and characteristics of both the transmitter and receiver were studied.

Ranging results were obtained that have potential for many applications. For example, under low attenuation conditions (≃0.6 dB/km), the experimental system was capable of ranging on laser-radar cross sections of $3.2 \times 10^{-2}$ $m^2$ at 5 km with an S/N-ratio of 39 dB. Moreover, under the same atmospheric conditions it had a maximum range on tree-

covered mountains of 32 km. A discrepancy that exists between the theoretical ranging performance and the preliminary measurements suggests that more investigation is needed to completely understand the system, target reflectivity and atmospheric characteristics.

One of the most promising potential applications of the TEA-$CO_2$ laser radar with heterodyne detection would be for a system designed to detect and track high-speed targets such as missiles and aircraft. At the present level of TEA-$CO_2$ laser technology, transmitters can operate at a repetition rate of a few hundred hertz and at peak power levels similar to those of the reported experimental system. The availability of commercial quadrant detectors having sufficient bandwidth to accomodate doppler frequency shifts from targets approaching at 1000 m/s enables the development of a sensitive receiver with the capability of discriminating between high-speed targets and clutter arising from the background and atmospheric backscatter. If channelized receiver or frequency tracking techniques were employed, the loss in the maximum range capability of the system would be insignifigant.

## 5.0 ACKNOWLEDGEMENTS

The author gratefully acknowledges the able technical assistance provided by J. Lemay, P. St-Pierre, G. Beaudin and R. Noël in the course of this work.

## 6.0 REFERENCES

1. Brandewie, R.A. and Davis, W.C. , "Parametric Study of a 10.6-μm Laser Radar", Appl. Opt., Vol. 12, pp. 1526-1533, July 1972.

2. Hughes, A.J. , O'shaughnessy, J. and Pike, E.R., "FM-CW Radar Range Measurement at 10-μm Wavelength", IEEE Journal of Quantum Electronics (Corresp.), Vol. QE-8 No. 12, pp. 909-910, December 1972.

3. Honeycutt, T.E. and Otto, W.F., "FM-CW Radar Range Measurement with a $CO_2$ Laser", IEEE Journal of Quantum Electronics (Corresp.), Vol. QE-8, pp. 91-92, February 1972.

4. Kingston, R.H. and Sullivan, L.J., "Coherent Laser Radar", Proceedings SPIE, Laser Systems, Vol. 69, pp. 10-13, 1975.

5. Gondhalekar, A., Holzhauer, E. and Heckenberg, N.R., "Single Longitudinal Mode Operation of High Pressure Pulsed $CO_2$ Lasers", Physics Letters, Vol. 46A, No. 3, pp. 229-230, 17 December 1973.

6. Girard, A., "The Effects of the Insertion of a CW, Low-Pressure $CO_2$ Laser into a TEA-$CO_2$ Laser Cavity", Optics Communications, Vol. 11, No. 4, pp. 346-351, August 1974.

7. Gondhalekar, A., Heckenberg, N.R, and Holzhauer, E., "The Mechanism of Single-Frequency Operation of the Hybrid-$CO_2$ Laser", IEEE Journal of Quantum Electronics, Vol. QE-11, No. 3, pp. 103-108, March 1975.

8. Cruickshank, J.M and Hale M.M., "Heterodyne Detection with TEA-$CO_2$ Hybrid Lasers". DREV R-4049/76, March 1976. UNCLASSIFIED

9. Teich, M.C., "Infrared Heterodyne Detection", Proceeding of the IEEE, Vol. 56, No. 1, pp. 1350-1356, January 1968.

10. Siegman, A.E., "The Antenna Properties of Optical Heterodyne Receivers", Proceedings of the IEEE, Vol. 54, No. 10, October 1966.

11. Fink, D., "Coherent Detection Signal-to-Noise", Applied Optics, Vol. 14, No. 3, pp. 689-690, March 1975.

12. Mandel, L. and Wolf, E., "Optimum Conditions for Heterodyne Detection of Light", Journal of the Optical Society of America, Vol. 65, No. 4, pp. 413420, April 1975.

13. Cohen S.C., "Heterodyne Detection: Phase Front Alignment, Beam Spot Size, and Detector Uniformity", Applied Optics, Vol. 14, No. 8, pp. 1953-1959, August 1975.